

# Well Test Analysis: Wells Producing by Solution Gas Drive

R. RAGHAVAN  
MEMBER SPE-AIME

U. OF TULSA  
TULSA, OKLA.

## ABSTRACT

*Drawdown and buildup data in a homogeneous, uniform, closed, cylindrical reservoir containing oil and gas and producing by solution gas drive at a constant surface oil rate were investigated. The well was assumed to be located at the center of the reservoir. Gravity effects were not included. Though the reservoir systems studied were assumed to be homogeneous, the effect of a damaged region in the vicinity of the wellbore was examined.*

Recently, alternate expressions for describing multiphase flow through porous media have been presented. These expressions incorporate changes in effective permeability and fluid properties (formation volume factor, viscosity, gas solubility) with pressure by means of a pseudopressure function. The validity of applying the pseudopressure-function concept to drawdown and buildup testing for multiphase-flow situations was investigated. The pseudopressure function for analyzing drawdown behavior is calculated differently from that required to analyze buildup data. Consequently, two pseudopressure functions are required for analysis of well behavior in multiphase-flow systems.

Dimensionless groups are used to extend the results to other situations having different permeabilities, spacing, reservoir thickness, well radii, porosity, etc., provided the PVT relations and relative-permeability characteristics are identical to those used in this study. The pseudopressure-function concept used to analyze drawdown and buildup behavior extends the applicability of the results to a wide range of PVT relations and relative-permeability characteristics.

## INTRODUCTION

During the past 30 years, more than 300 publications have considered various problems pertaining to well behavior. Except for a few (about 10), most papers examining transient pressure behavior assume that the fluids in the reservoir

obey the diffusivity equation. This implies the use of a single-phase, slightly compressible fluid. The reason for the popularity of this approach is twofold: (1) the ease with which the diffusivity equation can be solved for a wide variety of problems, and (2) the demonstration by some workers that, for some multiphase-flow situations, single-phase flow results may be used provided appropriate modifications are made. The necessary modifications are summarized in Ref. 1.

The main objective of this study is to present a method for rigorously incorporating changes in fluid properties and relative-permeability effects in the analysis of pressure data when two phases of oil and gas are flowing. This should enable the engineer to calculate the absolute formation permeability rather than the effective permeability to each of the flowing phases. This method is based on an idea suggested by Fetkovich,<sup>2</sup> who proposed that if an expression similar to the real gas pseudopressure is defined, then equations describing simultaneous flow of oil and gas through porous media may be simplified considerably. The validity of the equations and methods for calculating the pseudopressure function, however, was not presented by Fetkovich.

## LITERATURE REVIEW AND THEORETICAL CONSIDERATIONS

General equations of motion describing multiphase flow in porous media have been known since 1936.<sup>3,4</sup> These equations, and the assumptions involved in deriving them, are discussed thoroughly in the literature and will not be considered here.

Equations for two-phase flow were first solved by Muskat and Meres<sup>3</sup> for a few special cases. Evinger and Muskat<sup>5</sup> studied the effect of multiphase flow on the productivity index of a well and examined the steady radial flow of oil and gas in a porous medium. Under conditions of steady radial flow the oil flow rate is given by

$$q_o = \frac{kb}{141.2 \ln r_e/r} \int_p^{p_o} \frac{k_{ro}(S_o)}{\mu_o B_o} dp \dots (1)$$

Since relative permeability is a function of saturation, the integral in Eq. 1 can only be evaluated if a relationship between fluid saturation

Original manuscript received in Society of Petroleum Engineers office July 23, 1975. Paper accepted for publication Jan. 6, 1976. Revised manuscript received Feb. 17, 1976. Paper (SPE 5588) was first presented at the SPE-AIME 50th Annual Fall Technical Conference and Exhibition, held in Dallas, Sept. 28-Oct. 1, 1975. © Copyright 1976 American Institute of Mining, Metallurgical, and Petroleum Engineers, Inc.

This paper will be included in the 1976 Transactions volume.

and pressure is specified. This relationship is obtained from the gas-oil ratio (GOR) equation:

$$R = R_s + \frac{k_g \mu_o B_o}{k_o \mu_g B_g} \dots \dots \dots (2)$$

Perrine<sup>6</sup> proposed modifications to the single-phase flow theory to incorporate multiphase-flow effects. He suggested that the mobility term in the diffusivity equation be replaced by the sum of the mobilities of the individual phases and the total system compressibility by weighting the individual fluid compressibilities by the average saturation of that phase. This empirical approach was given a theoretical basis by Martin.<sup>7</sup> Using a high-speed digital computer, Weller<sup>8</sup> and Earlougher *et al.*<sup>9</sup> examined the buildup behavior for multiphase flow and demonstrated that Perrine's<sup>6</sup> approach is valid. However, Weller showed that, as the gas saturation increases, the analysis becomes less accurate.

The understanding of solution gas-drive reservoirs and well behavior was extended by Levine and Prats.<sup>10</sup> They showed that, if it is assumed that the decline rate of stock-tank oil in place is constant everywhere, then the equation governing flow of oil in radial coordinates can be directly integrated to give

$$\int_p^{p_e} \frac{k_{ro}(S_o)}{\mu_o B_o} dp = \frac{141.2 q_o}{kb} \left[ \frac{1}{2} \left( \frac{r^2 - r_e^2}{r_e^2} \right) - 2 \ln \frac{r}{r_e} \right] \dots \dots \dots (3)$$

As in the steady-state case, a relation between saturation and pressure is needed to calculate the integral on the left-hand side of Eq. 3. In addition, the pressure  $p_e$  and the corresponding saturation would have to be known.

To evaluate the pressure and saturation distributions using Eq. 3, Levine and Prats made two assumptions: (1) the GOR is constant everywhere and may be obtained from the Muskat<sup>11</sup> differential (tank) material-balance equations, and (2) the GOR corresponds to the pressure and saturation at the outer boundary.

More recently, using the analogy between gas and slightly compressible liquid flow, Fetkovich<sup>2</sup> presented expressions to describe transient, pseudosteady, and steady-state multiphase flow through porous media. He showed that in transient and pseudosteady-state multiphase flow the following equations should apply, respectively:

$$q_o = \frac{kb}{141.2(0.5 \ln t_D + 0.404 + s')} [m(p_i) - m(p_{wf})], \dots \dots \dots (4)$$

and

\*See Eq. 9 for definition of  $m_{wD}$ .

$$q_o = \frac{kb}{141.2(\ln 0.472 \frac{r_e}{r_w} + s')} [m(\bar{p}) - m(p_{wf})], \dots \dots \dots (5)$$

where  $m(p)$  is the pseudopressure function given by

$$m(p) = \int_{p_b}^p \frac{k_{ro}(S_o)}{\mu_o B_o} dp, \dots \dots \dots (6)$$

and  $t_D$  is the dimensionless time given by

$$t_D = \frac{0.000264 kt}{\phi \mu_{oi} c_{ti} r_w^2} \dots \dots \dots (7)$$

In Eqs. 4 and 5,  $s'$  is the skin effect and generally would include damage in the vicinity of the wellbore as well as an increased resistance caused by the development of a gas saturation; that is,  $s'$  is a function of the rate and time. Methods of calculating  $s'$  are given in Ref. 2. As already mentioned, Fetkovich<sup>2</sup> has not explicitly demonstrated the validity of the equations or presented a method to calculate the integral in Eq. 6. However, from a practical viewpoint, the equations represent an important advance in well test analysis because, with presently available techniques, only the effective permeability can be determined. Furthermore, a rigorous basis for commonly used drawdown and buildup methods for multiphase flow is established.

An important point regarding Eqs. 4 and 5 concerns the viscosity and compressibility values used in calculating the dimensionless-time group, for Eq. 7 indicates that initial system properties should be used. The rationale for this choice, based on the work of Aronofsky and Jenkins<sup>12</sup> and Al-Hussainy *et al.*,<sup>13</sup> will not be discussed here.

#### DETERMINATION OF THE PSEUDOPRESSURE FUNCTION

To use Eq. 4 or Eq. 5, the pressure and saturations must be related. This problem is more difficult than either the steady- or pseudosteady-state conditions examined by earlier workers. Furthermore, since the pseudopressure-function approach is used to analyze both drawdown and buildup data, it is not readily evident whether the same pseudopressure function should be used for both analyses. Undoubtedly, the  $m(p)$  function calculated to describe flow conditions at any point in the system should reflect both the saturation and the pressure gradients at that point.

During this investigation, several approaches were used to determine the pseudopressure function to correlate the drawdown solutions. The objective was to calculate the pseudopressure function such that a semilog graph of  $m_{wD}^*$  vs  $t_D$  would have a slope of 1.151 per log cycle during the early transient period for radial flow systems. It was

found that if the instantaneous producing GOR at the sand-face can be used to relate the pressure and saturation at the wellbore, then the above criterion would be satisfied. This method of calculating the pseudopressure function has no rigorous theoretical basis. It is recommended mainly on empirical grounds based on the results obtained. It also should be noted that this approach is substantially different from that used in Refs. 3 and 10.

It will be shown later that the pseudopressure function required to analyze buildup data must be calculated differently from that used to analyze drawdown data. For the present, it suffices to say that the use of separate pseudopressure functions implies that drawdown and buildup processes are not *exactly* reversible processes, a basic assumption of the single-fluid theory. Methods for calculating the pseudopressure function are given in the Appendix.

#### RESERVOIR CHARACTERISTICS AND ASSUMPTIONS

The PVT relations of the oil and gas used in this study are given in Fig. 1. Fig. 2 gives the relative-permeability relationships used. Most of the results presented in this paper correspond to the solid lines in Fig. 2. Some results corresponding to the dashed lines are presented to extend the applicability of the analysis. The initial reservoir pressure was assumed to be constant at a bubble-point pressure of 1,500 psi. Initially, the oil saturation was unity, with no interstitial water.

In all investigations the reservoir is assumed to be horizontal, homogeneous, and isotropic, and to

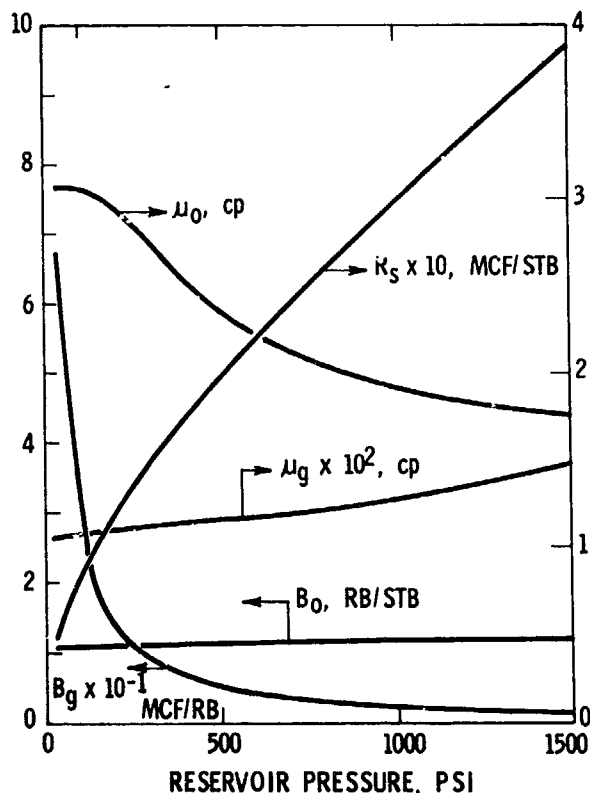


FIG. 1 — PVT RELATIONS OF OIL AND GAS.

TABLE 1 — RESERVOIR PROPERTIES AND FLOW GEOMETRIES

For all systems examined, the following reservoir and fluid properties are identical:

Porosity	0.119
Absolute permeability, md	6.16
Initial gas saturation	0
Initial water saturation	0
Initial pressure, psi	1,500
Initial system compressibility, psi <sup>-1</sup>	$1.335 \times 10^{-4}$
Initial oil viscosity, cp	1.7645
Initial gas viscosity, cp	0.0145

#### Reservoir Characteristics

Reservoir Dimensions		Well Radius (ft)	Flow Rates (STB/D)	Oil-in-Place (MSTB)
External Radius (ft)	Thickness (ft)			
500	25	0.5	10, 25	347.50
214.39	20	0.5	10, 25	63.95
214.39	25	0.5	40, 25	51.16

For all systems examined, abandonment condition is  $50 \pm 15$  psi.

be unaffected by gravity. Gravitational effects have been examined by Cook and Fulton.<sup>14</sup> In all cases, it is assumed that the producing well penetrates the formation fully.

Detailed information on each system examined here is given in Table 1. It is assumed that the reservoir produces at a constant surface oil rate. As gas is evolved, the solutions obtained should be sensitive to rate. Thus, rate variations were also examined. Computations were terminated when the wellbore pressure reached a low value of  $50 \pm 15$  psi. The termination of production at this wellbore pressure does not imply that the "economic limit" has been reached. It should be possible to hold the wellbore pressure at this value and allow the production rate to decline until an economic limit is reached. In this study, which is principally

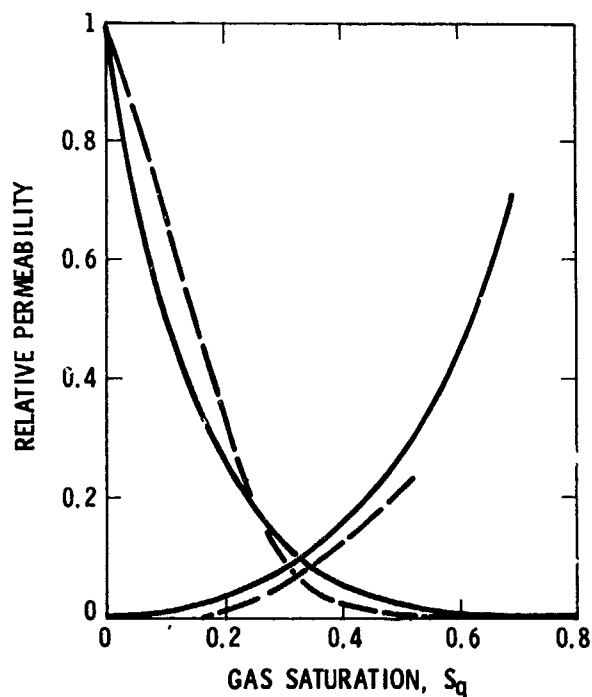


FIG. 2 — GAS-OIL RELATIVE-PERMEABILITY PROPERTIES OF THE RESERVOIR.

directed to short-time testing, the constant-terminal-pressure case has not been examined.

An important task of a well test analyst is to determine whether formation damage exists in the vicinity of the wellbore. As a result, the effect of wellbore damage on pressure behavior was studied. The skin effect considered in this paper implies a reduction in the permeability in the vicinity of the wellbore resulting from *physical changes* in the rock caused by invasion of drilling fluids, etc., and not the reduction in *flow capacity* resulting from gas buildup in the low-pressure regions.

## VALIDITY OF COMPUTER SOLUTIONS

The equations governing multiphase flow were solved using a two-phase numerical model available at the Amoco Research Center. This model includes implicit rates and implicit relative-permeability calculation procedures so as to increase model stability and provide for handling of large volumes of fluid throughput per block per time step.

An important consideration in the solution of finite-difference equations is the effect of discretization in space and time. The following procedure was adopted to insure that discretization errors did not affect the solutions obtained.

For each flow system considered, a set of fluid properties corresponding to a slightly compressible fluid was used to test the simulator. The results obtained were compared with the analytical solutions presented in the literature<sup>15</sup> over the *entire* flow period of interest. In all instances, the comparison between the finite-difference and analytical solutions was excellent (up to four significant figures on a dimensionless scale). The maximum value of the time step that could be used was also determined. (Note that this would also depend on the value of production time.) For the nonlinear case, the maximum time step used was less than one-half the value of the slightly compressible-fluid case at corresponding times. The time truncation error in this model is also controlled by limiting the maximum saturation change over a time step. If time-step lengths result in calculation of a saturation change greater than that specified (for a gas-oil problem this tolerance is 0.05), the program automatically generates subtime steps so that this limit is not exceeded.

A material-balance check was also used to insure that the solutions were accurate. Though material-balance checks are not an absolute indication of accuracy, they do insure that no serious errors are occurring and that the mass withdrawn would match the mean pressure decline.

## DIMENSIONLESS VARIABLES

For a slightly compressible liquid the range of validity of results obtained for a particular case can be extended by defining appropriate dimensionless variables. Since multiphase-flow equations depend on specific fluid and reservoir characteristics, solutions cannot be extended to

apply to all cases. However, results for one case can be extended to other values of absolute permeability, porosity, drainage, or well radius, provided the PVT properties of the crude, the relative permeabilities, and the initial and producing conditions remain unchanged. Thus, the dimensionless variables will be defined as follows. For the system under study, the dimensionless variables are<sup>15</sup>

Dimensionless Pressure Drop:

$$p_D(r_D, t_D) = \frac{kb}{141.2 q_o B_{oi} \mu_{oi}} [p_i - p(r, t)] \quad (8)$$

Dimensionless Pseudopressure Drop:

$$m_D(r_D, t_D) = \frac{kb}{141.2 q_o} [m(p_i) - m(r, t)] \quad (9)$$

Dimensionless Radial Coordinate:

$$r_D = r/r_w \quad (10)$$

The dimensionless time group is defined by Eq. 7.

The rationale for the choice of initial system properties in defining dimensionless time is discussed in Refs. 12 and 13. The choice of initial properties in the dimensionless-pressure function is mainly for convenience.

A dimensionless oil flow rate will aid discussion. This is defined by

$$q_{oD} = \frac{141.2 \mu_{oi} q_o}{kb p_i} \quad (11)$$

All the above are in field units. Field units are used consistently in the following. The units used are presented in the Nomenclature.

## RESULTS AND CORRELATIONS

In the following discussion, both drawdown and buildup results are presented.

### PRESSURE BEHAVIOR AT THE WELLBORE (DRAWDOWN)

Fig. 3 is a conventional semilog graph presenting the pressure behavior of a well producing under solution gas drive and located at the center of a closed, circular reservoir. The solid lines in Fig. 3 correspond to solutions that would be obtained for the slightly compressible-liquid case. A well producing a slightly compressible fluid and not located on the drainage boundary of a closed shape experiences three stages of depletion: an early transient period, a transition period, and a pseudosteady flow period. During the early transient period, the dimensionless pressure drop is a linear function of the logarithm of dimensionless time,

$t_D$  with a slope equal to 1.151 per log cycle. No effect of the drainage boundary is evident during this period. For the problem under consideration, the duration of the late transient period is negligible.<sup>16</sup> The early transient and pseudosteady-state flow periods in Fig. 3 refer to  $r_e/r_w = 428.8$  only.

Examination of the solution gas drive data in Fig. 3 indicates that the early-time drawdown data have a slight curvature with an increasing slope. The increase in slope can be explained by noting that a gas saturation develops during this time resulting in a decrease in the permeability to oil. The decrease in effective permeability is reflected by an increase in slope of the drawdown curve. Since gas would be evolved more rapidly at higher flow rates, the slope of the curve should increase as the flow rate increases.

All wells at any location in a closed reservoir eventually will exhibit a pseudosteady-state period. During this period the dimensionless wellbore pressure drop is a linear function of dimensionless time. For a slightly compressible fluid a plot of  $p_{wD}$  vs  $t_{DA}$  has a slope of  $2\pi$  for  $t_{DA} > 0.1$ , where  $t_{DA}$ , the dimensionless time based on drainage area, is related to  $t_D$  by

$$t_{DA} = \frac{r_w^2 t_D}{\pi r_e^2} \dots \dots \dots (12)$$

The late-time data for some of the cases shown in Fig. 3 are replotted on Cartesian coordinates in Fig. 4. The results indicated that the late-time data may be approximated by straight-line segments for a considerable length of time. However, not all these straight-line sections have a slope equal to  $2\pi$ . Thus, care should be taken in interpreting reservoir limit tests if gas saturation effects are dominant, since theoretical developments assume that the slope of the pressure-time graph in the pseudosteady-state region is equal to  $2\pi$ . At this stage an important aspect of the results shown in Fig. 3 should be noted. From close examination of the data indicated by triangles and circles, it may

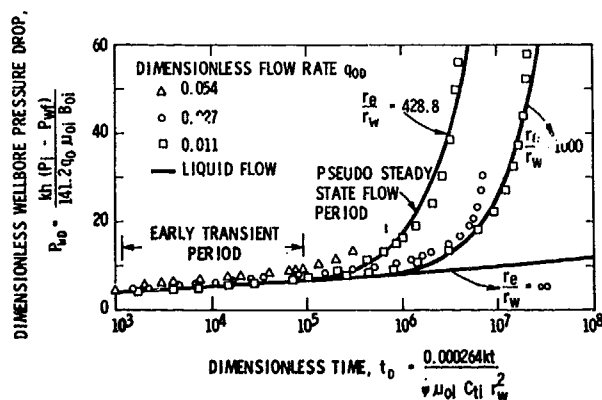


FIG. 3 — DIMENSIONLESS WELLBORE PRESSURE DROP,  $p_{wD}$ , VS DIMENSIONLESS TIME,  $t_D$ .

appear that they do not extend over a very long flow period and that flow behavior in the pseudosteady-state flow period has not been investigated. Actually, this is not so. The last point shown in Fig. 3 corresponds to a producing pressure of about 50 psi for each flow rate.

So far, the general characteristics of drawdown behavior have been examined conventionally. The advantages of using the pseudopressure function proposed by Fetkovich<sup>2</sup> will now be discussed. Fig. 5 is a conventional semilog graph of the dimensionless pseudopressure at the well,  $m_{wD}$ , vs dimensionless time,  $t_D$ . The triangular, square, and circular data points are results of this study. The solid line (which appears to be drawn through these points in the early-time range) is the constant-property solution<sup>15</sup> ( $p_{wD}$  vs  $t_D$ ). The GOR curve used to calculate the pseudopressure function is shown in Fig. 6. The procedure for calculating the pseudopressure is outlined in the Appendix.

A comparison of  $m_{wD}$  with  $p_{wD}$  values indicates that the difference between the two solutions is negligible during the early transient period. Of more importance, the slope of  $m_{wD}$  vs  $t_D$  is identical to that of  $p_{wD}$  vs  $t_D$  over the entire early transient range. This is the basis for calculating the

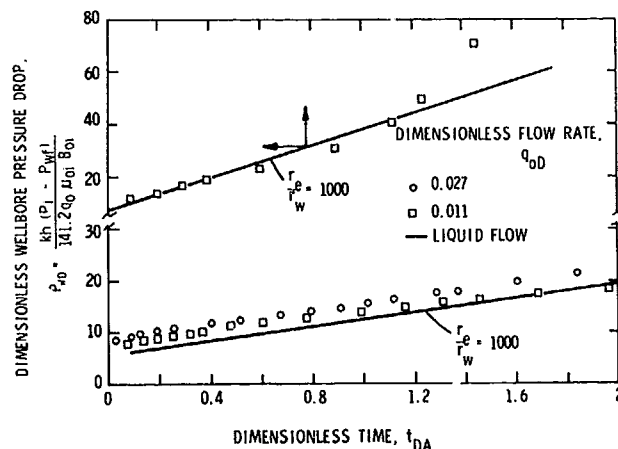


FIG. 4 — DIMENSIONLESS WELLBORE PRESSURE DROP,  $p_{wD}$ , VS DIMENSIONLESS TIME,  $t_{DA}$ .

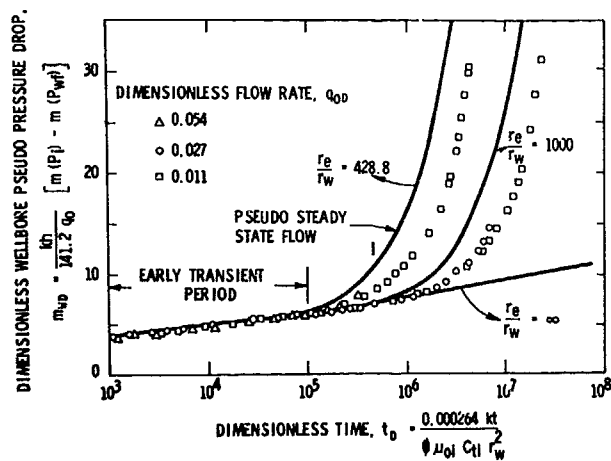


FIG. 5 — DIMENSIONLESS PSEUDOPRESSURE DROP,  $m_{wD}$ , VS DIMENSIONLESS TIME,  $t_D$ .

pseudopressure function by the approach suggested in this paper. Thus, from a practical viewpoint, the *absolute* formation permeability can be obtained from the slope of the drawdown curve if the pseudopressure function is used. It also should be noted that the use of the pseudopressure function eliminates the effect of rate over virtually all the production history.

Departure from the van Everdingen and Hurst<sup>15</sup> solutions occurs for large values of  $t_D$  when boundary effects are felt. The trend of the departure is in the same direction as the real gas flow correlations of Al-Hussainy *et al.*<sup>13</sup> However, one difference between the real gas flow correlations and present results should be noted. For the cases examined in this study, the  $m_{wD}$  correlation is not rate sensitive, whereas the natural gas correlations are. This does not imply that the terminal producing pressure is reached at the same time for all producing rates. It implies that, for the problem under consideration,  $m_{wD}$  values *will not* approach  $p_{wD}$  values as the rate is reduced.

It was pointed out earlier that, for the systems examined, late-time data of  $p_{wD}$  vs  $t_{DA}$  do not form straight lines with a slope equal to  $2\pi$ . This observation is also applicable if data are converted in terms of pseudopressures. Though apparent straight lines result, the slope of the straight lines is much less than  $2\pi$  (Fig. 7).

An interesting feature of the drawdown solutions obtained in this study is the role of the gas saturation in the vicinity of the wellbore. Many

workers have viewed gas saturation as a skin effect. This view is reasonable and is substantiated by the data in Fig. 3. However, if the pseudopressure function is used, the incorporation of a skin effect to account for the gas saturation is not necessary, since the dimensionless pseudopressure is never greater than the dimensionless pressure drop for a slightly compressible fluid. Thus, the concept of a *time-dependent skin effect* appears to be *unnecessary* if the pseudopressure function is used.

Fetkovich<sup>2</sup> has proposed that the transient drainage-radius concept introduced by Aronofsky and Jenkins also should apply to multiphase flow. The transient drainage radius,  $r_d$ , is given by

$$\ln \frac{r_d}{r_w} = m_D(1, t_D) - m_D(\bar{p}, t_D), \dots (13)$$

where  $m_D(\bar{p}, t_D)$  is the dimensionless pseudopressure drop corresponding to the average pressure.

Eq. 15 implies that, if the average pressure is determined from material balance, then the drainage radius of the well can be calculated. A basic problem still remains, however. This pertains to determination of  $m(\bar{p})$ . If the procedure to determine  $m_{wD}(t_D)$  is followed, then the GOR at the average pressure point has to be determined. It is possible to obtain this information from a simulator. However, in practical situations this would not be possible. In that event, it is recommended that the producing GOR be used. This implies that the GOR is constant everywhere. This is a reasonable assumption for long times.

The  $m(\bar{p})$  function was calculated using both methods outlined above. It was found that the drainage-radius correlation agreed fairly well with liquid-flow results and was better than the  $m_{wD}$  vs  $t_D$  correlation shown in Fig. 5 for large times. However, it is not as good as the gas flow correlations presented in Refs. 12 and 13. This correlation may be used in the manner suggested in Refs. 12 and 13 to calculate approximate the drainage radius.

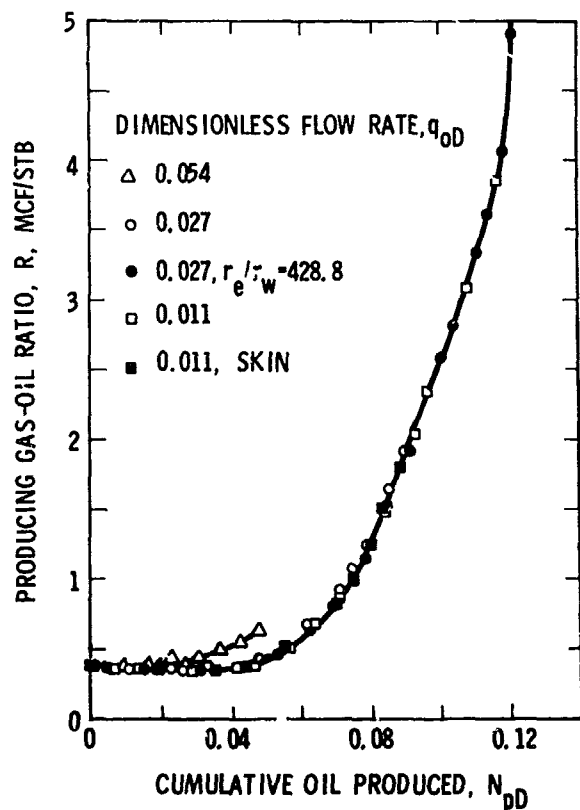


FIG. 6 — PRODUCING GOR VS CUMULATIVE OIL PRODUCED (RADIAL SYSTEM).

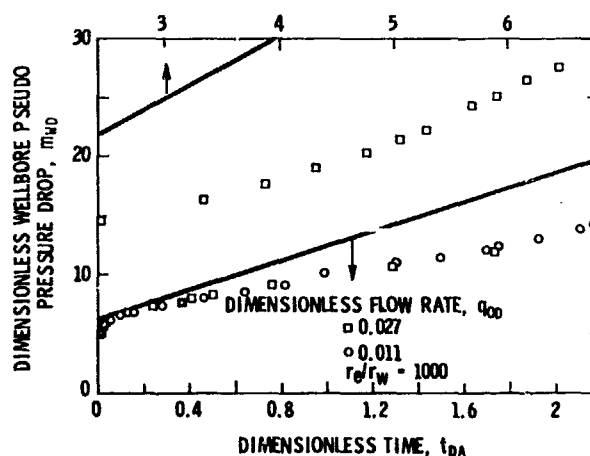


FIG. 7 — DIMENSIONLESS WELLBORE PSEUDOPRESSURE DROP,  $m_{wD}$ , VS DIMENSIONLESS TIME,  $t_{DA}$ .

## BUILDUP TESTING

Theoretical and practical experience has shown<sup>1,6-9</sup> that methods of analysis applicable to flow of slightly compressible liquids may be applied to wells producing by solution gas drive provided the modifications discussed by Perrine<sup>6</sup> are incorporated. In the following, application of the pseudopressure concept to buildup testing is presented.

### DETERMINATION OF THE PSEUDOPRESSURE FUNCTION DURING PRESSURE BUILDUP

Before discussing the quantitative results, a discussion of the application of the pseudopressure function to buildup testing is warranted. Several important questions, as well as assumptions, arise in applying this concept to buildup testing. Analysis of buildup data by the pseudopressure function for buildup analysis is presented in the following two methods. The first method assumes the pseudopressure-pressure relationship developed for drawdown is also applicable to buildup testing. Fundamentally, this implies that buildup and drawdown are *reversible* processes and, thus, the concept of superposition may be used. In a manner analogous to drawdown situations, the true absolute formation permeability should be obtained from the slope of the buildup straight line if the drawdown function,  $m(p)$ , is applicable. If this method is used, then calculated values of formation permeability were a function of producing time (gas saturation). This implies that buildup and drawdown are not strictly reversible processes. Accordingly, other methods for evaluating the  $m(p)$  function during buildup were considered. The rationale for calculating the  $m(p)$  function for *buildup* finally used is as follows.

Fundamentally, the pressure rise at the wellbore reflects conditions at points within the area drained by the well, and the pressure buildup curve of a well should reproduce nearly exactly the same pressure profile that existed in the reservoir at the instant of shut-in. Thus, any circumstance that affects or modifies the pressure profile should be expected to modify or affect the buildup trace. For systems examined in this study, the buildup behavior is a function not only of the pressure distribution, but also of the saturation distribution, formation relative-permeability characteristics, and fluid properties. The  $m(p)$  function used to analyze buildup should reflect conditions occurring during buildup in the reservoir. Again, the GOR at the instant of shut-in is a representative measure of the conditions prevailing in the area drained by the well. Thus, the second method for calculating the pseudopressure function for buildup assumes that the GOR is constant during the buildup period and is equal to the producing GOR at the instant of shut-in. Basically, this implies that the pressure changes occur much faster in the reservoir than the time interval in which large changes in saturation take place. The above discussion is based on essentially intuitive grounds, though

available evidence<sup>8,10</sup> indicates that at large times the GOR may be assumed to be a constant.

In this following analysis of buildup data using both methods, it should be noted that the two  $m(p)$  functions are independent of each other. It will be shown that the second method is preferable to the first.

### PRESSURE BEHAVIOR AT THE WELL (BUILDUP)

Buildup behavior of radial reservoirs for two stages of depletion are examined to demonstrate the effects of gas saturation. Results obtained by conventional methods suggested in the literature are not considered in detail here.

Fig. 8 is a semilog graph<sup>17</sup> of buildup data corresponding to two stages of depletion ( $t = 60$  and 1,240 days) using the "drawdown" pseudopressure function. The slope of the straight lines should be inversely proportional to the *absolute* permeability-thickness product of the medium if the drawdown pseudopressure function is applicable to buildup cases. The calculated values of the absolute permeability-thickness products are shown in Fig. 8. The  $kh$  values obtained are lower than the actual absolute permeability-thickness product (154 md-ft). As the difference increases with producing time, it appears that the liberation of gas affects the analysis of buildup data by this approach. This also may be because the drawdown  $m(p)$  correlation is not very good for large values of producing time.

The buildup data shown in Fig. 8 have been replotted in Fig. 9 using the shut-in pseudopressure function. Calculated values of permeability-thickness are within the engineering accuracy of the simulator input value for both producing times. Based on the results shown in Fig. 9 and others not presented here, it appears that this approach is better than the drawdown pseudopressure-function

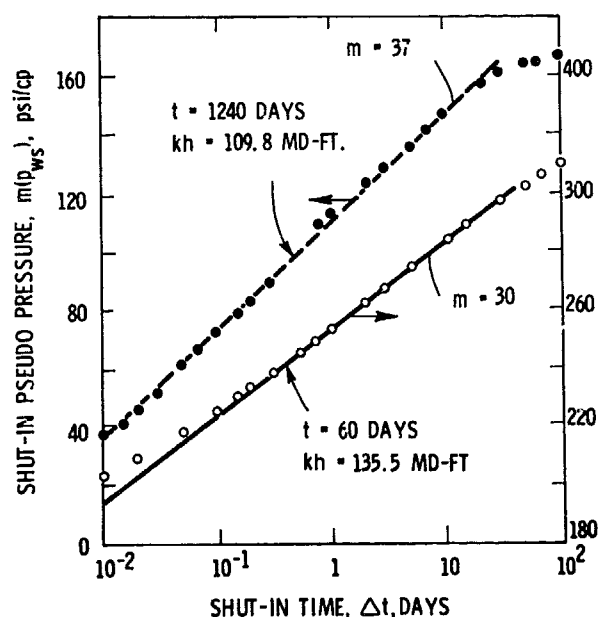


FIG. 8 — BUILDUP ANALYSIS IN A RADIAL SYSTEM USING DRAWDOWN PSEUDOPRESSURE FUNCTION.

approach. The results in Fig. 9 indicate that this concept can be used to determine the absolute permeability-thickness of the formation within acceptable accuracy in spite of the change in oil and gas saturations in the flow system under consideration. A sample calculation of obtaining the pseudopressure function is given in the Appendix.

An important consequence of using different  $m(p)$  functions for buildup and drawdown also should be noted. For gas reservoirs, a single graph of  $m(p)$  vs  $p$  will be applicable for the entire life of the reservoir. In the present instance, this is not so since the pseudopressure function is dependent on the producing GOR and producing rate at the instant the well is shut in. Thus, a family of  $m(p)$  vs  $p$  curves would be required to analyze data at various times during the life of the reservoir. Each curve would correspond to a specific GOR.

#### THE SKIN EFFECT — DRAWDOWN

In this study, the skin effect was represented by an annular region surrounding the wellbore. The

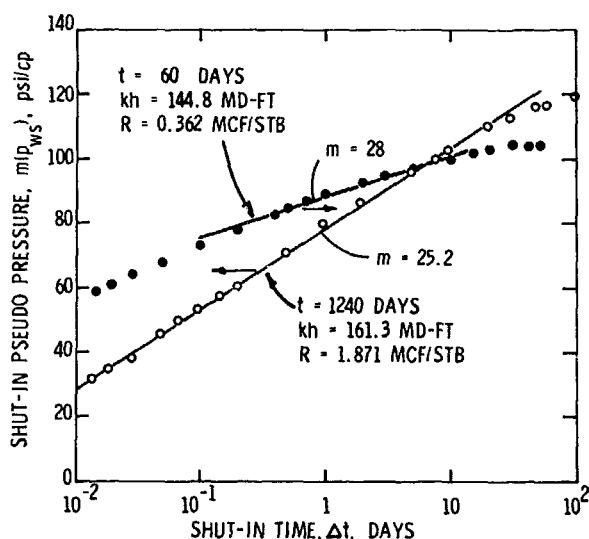


FIG. 9 — BUILDUP ANALYSIS IN A RADIAL SYSTEM USING SHUT-IN PSEUDOPRESSURE FUNCTION.

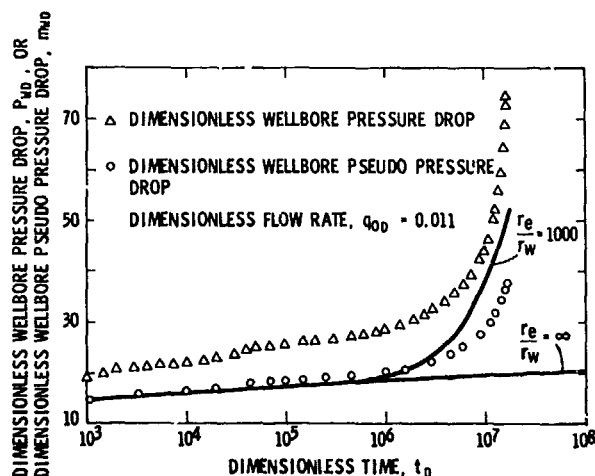


FIG. 10 — DIMENSIONLESS WELLBORE PRESSURE DROPS ( $p_{wD}$  OR  $m_{wD}$ ) VS DIMENSIONLESS TIME,  $t_D$  (RADIAL SYSTEM WITH SKIN).

permeability-thickness of the skin region was assumed to be a fraction of the formation permeability-thickness; that is, only damage was considered. In the results presented in this study, the skin region extends to a distance of 1.7 ft from the axis of the wellbore and permeability-thickness in this region is 1/10 the permeability-thickness of the reservoir. This corresponds to a steady-state infinitesimal skin effect,  $s \approx 11$ .

Fig. 10 is a conventional semilog graph of the pressure behavior of a composite radial system. The solid line in Fig. 10 corresponds to the slightly compressible-fluid case and includes the effect of the damaged region.

The triangular data shown in Fig. 10 represent the drawdown data ( $p_{wD}$  vs  $t_D$ ) corresponding to the solution-gas case. The deviations in the straight line from the early portion are principally caused by the change in gas saturation. The difference between the solid line and the triangular points reflects the increase in pressure drop owing to gas liberation. For the case under study, this effect is much more predominant than the zero-skin case.

The circular points in Fig. 10 are a replot of the triangular data using the pseudopressure function. The relationship of GOR vs cumulative oil produced used to obtain the circular points is shown in Fig. 6. The correlation between the two solutions is excellent during the transient period. For large times the two solutions depart in a manner similar to the zero-skin case. This correlation amply demonstrates the applicability of the pseudopressure concept to account for wellbore damage in radial systems.

#### THE EFFECT OF RELATIVE PERMEABILITY

The objective of introducing the pseudopressure-function concept to drawdown and buildup testing was to present a method of analysis that would be applicable to a wide range of PVT properties and relative-permeability characteristics. To provide some justification for use of the pseudopressure function in drawdown and buildup testing, drawdown results using one other set of relative-permeability data for a well at the center of a closed radial reservoir producing at a constant surface rate are presented. The relative-permeability data used are shown as dashed lines in Fig. 2.

Fig. 11 presents the dimensionless drawdown data for a well producing at a constant surface rate from a closed radial reservoir. The solid line corresponds to the flow of a slightly compressible fluid. The square data points reflect the pressure behavior for the solution gas-drive case. The circular data points are results obtained when the pseudopressure function is used. The GOR relationship used to obtain the pseudopressure function is shown in Fig. 12. As in Fig. 5, during the early transient period the slope of  $m_{wD}$  vs  $t_D$  is identical to  $p_{wD}$  vs  $t_D$ . This implies that the absolute formation permeability can be obtained from the slope of the drawdown graph. The long-time behavior of  $m_{wD}$  vs  $t_D$  is different from the data



presented in Fig. 5 and reflects the different relative-permeability characteristic of the porous medium. Thus, no single set of  $m_{wD} - t_D$  data can be expected to apply at long production times.

These data should provide some justification for the extension of the results to other systems through the use of the pseudopressure function.

## CONCLUSIONS

The main objective of this paper was to determine the applicability and utility of the pseudopressure-function approach to drawdown and buildup testing. Methods for calculating this function have been discussed. It has been shown that the producing GOR may be used to relate the pressure and saturation terms that occur in the pseudopressure function. Furthermore, solution gas-drive drawdown data may be correlated with liquid-flow solutions for producing times before pseudosteady-state production. This correlation is also applicable if the well is damaged. In many respects, this result is similar to the real gas pseudopressure-function correlation commonly used in gas well testing. However, one important difference exists. For gas reservoirs, buildup behavior may be analyzed as one set of  $m(p)$  vs  $p$  data throughout the life of the reservoir. For two-phase flow, a  $m(p)$  vs  $p$  graph would have to be obtained for each buildup test, since  $m(p)$  depends on the producing GOR at the instant the well is shut in and on producing rate. From a practical viewpoint, the results imply that the *absolute* formation permeability can be calculated from drawdown data if the pseudopressure function is used.

In the course of this investigation, it was found that the pseudopressure function used to analyze drawdown data is not adequate for interpreting buildup data. Accordingly, an alternate method of calculating the pseudopressure function to analyze buildup data is presented. The pseudopressure function is calculated on the producing GOR at the

instant of shut-in. This is very convenient since the history of the well over long time periods need not be taken into account. As in the drawdown case, the *absolute* formation permeability can be calculated by the pseudopressure-function approach for all gas saturations.

The use of two pseudopressure functions implies that drawdown and buildup are not exactly reversible processes — a fundamental assumption in classical well test analysis. In this respect, this paper constitutes a departure from existing theories.

## NOMENCLATURE

- $A$  = area, sq ft
- $B$  = formation volume factor, RB/STB, Mcf/RB
- $c_t$  = total system compressibility, psi<sup>-1</sup>
- $b$  = thickness of the formation, ft
- $k$  = absolute permeability, md
- $k_{rg}(S_0)$  = relative permeability to gas
- $k_{ro}(S_0)$  = relative permeability to oil
- $m(p)$  = pseudopressure, psi/cp
- $m_D(r_D, t_D)$  = dimensionless pseudopressure drop
- $p$  = fluid pressure, psi
- $p_D(r_D, t_D)$  = dimensionless pressure drop
- $p_e$  = pressure at the external boundary, psi
- $p_i$  = initial pressure in the system, psi

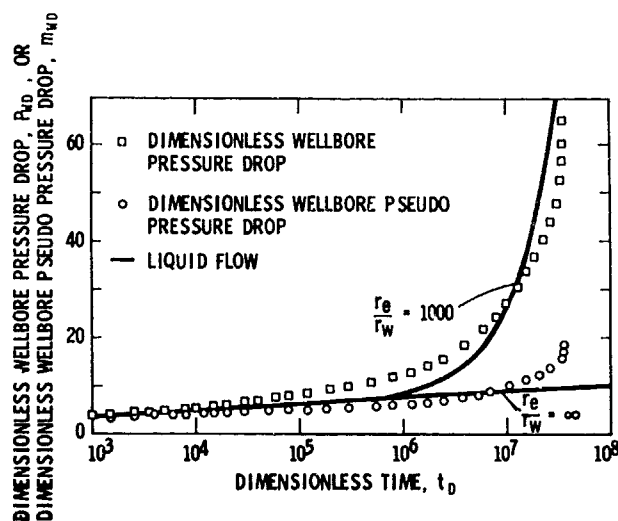


FIG. 11 — DIMENSIONLESS WELLBORE PRESSURE DROPS ( $p_{wD}$  OR  $m_{wD}$ ) VS DIMENSIONLESS TIME,  $t_D$ .

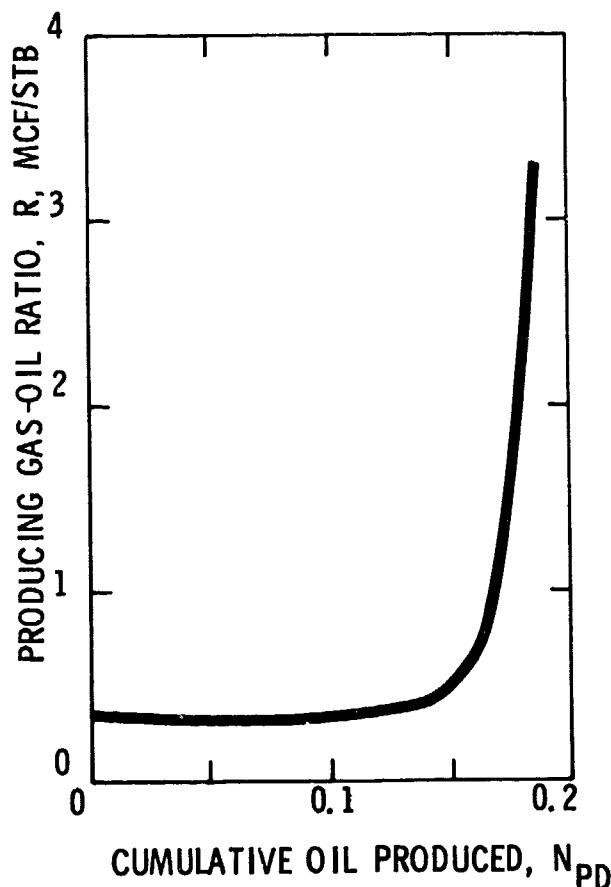


FIG. 12 — PRODUCING GOR VS CUMULATIVE OIL PRODUCED.

$p_{wf}$  = flowing well pressure, psi  
 $p_{ws}$  = shut-in well pressure, psi  
 $p_{wf,s}$  = flowing pressure at instant of shut-in, psi  
 $\bar{p}$  = average pressure in the system, psi  
 $q_o$  = surface oil flow rate, STB/D  
 $q_{oD}$  = dimensionless flow rate  
 $r$  = radius, ft  
 $r_d$  = Aronofsky-Jenkins drainage radius, ft  
 $r_D$  = dimensionless radial distance  
 $S$  = saturation, dimensionless  
 $t$  = time, hours or days  
 $t_D$  = dimensionless time based on wellbore radius  
 $t_{DA}$  = dimensionless time based on drainage area  
 $\Delta t$  = shut-in time, hours or days  
 $R$  = producing GOR, SCF/STB or Mcf/STB  
 $R_s$  = solution GOR, SCF/STB or Mcf/STB  
 $s$  = skin effect  
 $x$  = distance, ft  
 $\phi$  = porosity  
 $\mu$  = viscosity

#### SUBSCRIPTS

$e$  = external radius  
 $g$  = gas  
 $i$  = initial  
 $o$  = oil  
 $w$  = well  
 $wf$  = well flowing

#### ACKNOWLEDGMENTS

I take this opportunity to express my appreciation John L. Yanosik for providing me with his expertise in model runs. Conversations with Del D. Fussell regarding the pseudopressure-function approach are acknowledged. H. N. Hall, R. D. Carter, and R. G. Agarwal made a number of valuable suggestions that improved the quality of this manuscript. I am also thankful to Amoco Production Co. for permission to present this paper.

#### REFERENCES

1. Matthews, C. S. and Russell, D. G.: *Pressure Buildup and Flow Tests in Wells*, Monograph Series, Society of Petroleum Engineers, Dallas (1967) Vol. 1, 163.
2. Fetkovich, M. J.: "The Isochronal Testing of Oil Wells," paper SPE 4529 presented at the SPE-AIME 48th Annual Fall Meeting, Las Vegas, Nev., Sept. 30-Oct. 3, 1973.
3. Muskat, M. and Meres, M. W.: "The Flow of Heterogeneous Fluids Through Porous Media," *Physics* (Sept. 1936) Vol. 7, 346-363.
4. Wycoff, R. D. and Botset, H. G.: "The Flow of Gas-Liquid Mixtures Through Unconsolidated Sands," *Physics* (Sept. 1936) Vol. 7, 325-345.
5. Evinger, H. H. and Muskat, M.: "Calculation of Theoretical Productivity Factor," *Trans., AIME* (1942) Vol. 146, 126-139.
6. Perrine, R. L.: "Analysis of Pressure Buildup Curves," *Drill. and Prod. Prac.*, API (1956) 482.
7. Martin, J. C.: "Simplified Equations of Flow in Gas Drive Reservoirs and the Theoretical Foundation of Multiphase Pressure Buildup Analyses," *Trans., AIME* (1959) Vol. 216, 309-311.
8. Weller, W. T.: "Reservoir Performance During Two-Phase Flow," *J. Pet. Tech.* (Feb. 1966) 240-246; *Trans., AIME*, Vol. 237.
9. Earlougher, R. C., Jr., Miller, F. G., and Mueller, T. D.: "Pressure Buildup Behavior in a Two-Well Gas-Oil System" *Soc. Pet. Eng.* (June 1967) 195-204; *Trans., AIME*, Vol. 240.
10. Levine, J. S. and Prats, M.: "The Calculated Performance of Solution-Gas-Drive Reservoirs," *Soc. Pet. Eng. J.* (Sept. 1961) 142-152; *Trans., AIME*, Vol. 222.
11. Muskat, M.: "The Production Histories of Oil Producing Gas-Drive Reservoirs," *J. Applied Phys.* (March 1945) 147-159.
12. Aronofsky, J. S. and Jenkins, R.: "A Simplified Analysis of Unsteady Radial Gas Flow," *Trans., AIME* (1954) Vol. 201, 149-154.
13. Al-Hussainy, R., Ramey, H. J., Jr., and Crawford, P. B.: "The Flow of Real Gases Through Porous Media," *J. Pet. Tech.* (May 1966), 624-636; *Trans., AIME*, Vol. 237.
14. Cook, R. E. and Fulton, P. F.: "The Effects of Production Rate and Completion Interval on the Natural Depletion Performance of Massive-Sand Oil Reservoirs," paper SPE 4631 presented at the SPE-AIME 48th Annual Fall Meeting, Las Vegas, Nev., Sept. 30-Oct. 3, 1973.
15. van Everdingen, A. F. and Hurst, W.: "The Application of the Laplace Transformation to Flow Problems in Reservoirs," *Trans., AIME* (1949) Vol. 186, 305-324.
16. Ramey, H. J., Jr., and Cobb, W. M.: "A General Pressure Buildup Theory for a Well in a Closed Drainage Area," *J. Pet. Tech.* (Dec. 1972) 1493-1505; *Trans., AIME*, Vol. 251.
17. Miller, C. C., Dyes, A. B., and Hutchinson, C. A., Jr.: "The Estimation of Permeability and Reservoir Pressure From Bottom-Hole Pressure Build-Up Characteristics," *Trans., AIME* (1950) Vol. 189, 91-104.

#### APPENDIX

##### DETERMINATION OF PSEUDOPRESSURE FUNCTIONS

In this section methods for calculating both pseudopressure functions are discussed. An example problem is presented to provide detailed calculations.

##### PROCEDURE FOR CALCULATING $m(p)$ VS $p$ FOR DRAWDOWN

As mentioned in the text, the procedure for calculating the  $m(p)$  vs  $p$  relation uses the producing GOR. The following procedure is recommended.

1. Tabulate  $t$ ,  $p$ , and  $R$  in appropriate units.
2. Using tabulated values of  $p$  and  $R$ , calculate  $k_g/k_o$  using Eq. 2.
3. From relative-permeability curves calculate  $k_g/k_o$  as a function of  $S_o$  (or  $S_g$ ).
4. From Steps 2 and 3 determine  $p$  vs  $S_o$ .
5. From knowledge of  $p$  vs  $S_o$  obtain  $k_{ro}$  vs  $p$

using relative-permeability data.

6. Calculate  $m(p)$  (Eq. 6) by the trapezoidal rule on any other integration procedure using the relation in Step 5 and PVT data. Thus, we have the  $m(p)$  vs  $p$  curve for drawdown.

7. This curve may be used to convert all pressures to pseudopressures.

8. The pseudopressure vs time data then may be converted to dimensionless form.

#### PROCEDURE FOR CALCULATING $m(p)$ VS $p$ FOR BUILDUP

The following procedure is recommended. It is similar to the drawdown case except that a single value of  $R$  is used for all pressures.

1. From the producing GOR at the instant of shut-in, calculate the relationship between  $k_g/k_o$  and pressure using Eq. 2 (Keep in mind that, in this computation, the left-hand side of Eq. 2 is a constant.)

2. From relative-permeability curves calculate  $k_g/k_o$  vs  $S_o$  (or  $S_g$ ).

3. From Steps 1 and 2 obtain  $p$  vs  $S_o$ .

4. From a knowledge of  $p$  vs  $S_o$  obtain  $k_{ro}$  vs  $p$  using relative permeability data. (This will apply only to the *buildup* under question.)

5. Calculate  $m(p)$  (Eq. 6) by the trapezoidal rule or any other integration procedure using the relationship in Step 5 and PVT data. Thus, we have  $m(p)$  vs  $p$  for *buildup*.

TABLE 2 — FLOWING PRESSURE,  $p_{wf}$ , VS OIL SATURATION AT SAND-FACE,  $S_o$ .

Flow rate, $q_o$ , STB/D	10
Thickness, $h$ , ft	25
Reservoir radius, $r_e$ , ft	214.39
Relative-permeability data:	Solid line in Fig. 2
Oil Saturation at Sand-Face, $S_o$	Flowing Pressure, $p_{wf}$ (psi)
0.692	40.000
0.703	62.000
0.714	84.000
0.731	111.736
0.776	215.080
0.794	316.517
0.813	403.918
0.832	474.891
0.843	534.785
0.857	648.322
0.865	699.013
0.877	786.406
0.888	856.337
0.897	911.838
0.905	959.805
0.913	1,001.495
0.924	1,071.841
0.928	1,120.235
0.929	1,168.634
0.929	1,215.577
0.929	1,296.750
0.930	1,359.199
0.930	1,381.604
0.930	1,410.711
0.943	1,415.552
0.958	1,420.259
0.970	1,426.326
0.977	1,451.899
0.996	1,479.110
1.000	1,500.000

6. The data then may be analyzed along the lines shown below.

#### EXAMPLE PROBLEM

Pseudopressure functions for calculating drawdown and buildup are presented. As mentioned in the text, it should be noted that  $m(p)$  must be calculated differently for drawdown and buildup.

#### Drawdown

Using the procedure detailed above, the producing GOR (Fig. 6) vs pressure curve, obtained from the simulator, was first converted to a saturation vs pressure curve. These data are shown in Table 2. Then, using PVT data (Fig. 1) and data shown in Table 2,  $p$  vs  $m(p)$  was obtained (Table 3).  $m(p)$  was calculated by the trapezoidal rule. This relation was then used to convert all the pressure data in terms of pseudopressure (Table 4).

#### Buildup

The procedure is similar to that of drawdown; however, the producing GOR is assumed to be constant and a relationship between  $S_o$  and  $p_{ws}$  is obtained from Eq. 3 in the manner outlined above. Together with this relationship and PVT data, the  $m(p)$  integral may be obtained using trapezoidal rules;  $m(p_{ws})$  vs  $p_{ws}$  is tabulated in Table 5. The buildup data are given in Table 6. Also shown in Table 6 are sample calculations. It is emphasized that the results in Table 5 apply only to the pro-

TABLE 3 — DRAWDOWN PSEUDOPRESSURE VS FLOWING PRESSURE,  $p_{wf}$

Flowing Pressure, $p_{wf}$ (psi)	Drawdown Pseudopressure, $m(p_{wf})$ (psi/cp)
50	0.0
75	0.9594
100	2.0483
150	4.6231
200	7.7296
250	11.3670
300	15.3494
350	19.6802
400	24.4711
450	29.8491
500	35.8874
550	42.4557
600	49.4471
650	56.9118
700	64.9677
750	73.6264
800	82.8488
850	92.6937
900	103.2064
950	114.4065
1,000	126.4162
1,050	139.2528
1,100	152.7897
1,150	166.7654
1,200	180.9512
1,250	195.2371
1,300	209.5905
1,350	224.0493
1,400	238.6213
1,450	257.0068
1,500	279.3491

TABLE 4 — DIMENSIONLESS WELLBORE PSEUDOPRESSURE DROP,  $m_{wD}$ , VS DIMENSIONLESS TIME,  $t_D$ 

Dimensionless Time, $t_D$	Flowing Pressure, $p_{wf}$ (psi)	Pseudopressure, $m(p_{wf})$ (psi/cp)	Pseudopressure, Change, $\Delta m$ (psi/cp)	Dimensionless Wellbore Pseudopressure, $m_{wD}$
$2.930 \times 10^3$	1,410.663	242.234	37.115	4.048
$3.800 \times 10^3$	1,407.323	241.103	38.246	4.171
$5.090 \times 10^3$	1,403.518	239.813	39.536	4.312
$6.490 \times 10^3$	1,399.627	238.512	40.837	4.454
$1.000 \times 10^4$	1,392.636	236.472	42.877	4.676
$1.501 \times 10^4$	1,386.187	234.590	44.759	4.882
$3.980 \times 10^4$	1,370.046	237.058	49.291	5.376
$4.950 \times 10^4$	1,367.095	229.024	50.325	5.489
$8.509 \times 10^4$	1,356.246	225.867	53.482	5.833
$1.406 \times 10^5$	1,350.885	224.307	55.042	6.003
$2.354 \times 10^5$	1,320.098	215.389	63.960	6.976
$3.633 \times 10^5$	1,294.47	208.001	71.348	7.782
$4.321 \times 10^5$	1,281.178	204.181	75.168	8.198
$5.103 \times 10^5$	1,267.409	200.229	79.120	8.629
$8.529 \times 10^5$	1,210.247	183.875	95.474	10.413
$1.155 \times 10^6$	1,164.373	170.833	108.516	11.835
$1.682 \times 10^6$	1,088.911	149.755	129.594	14.134
$2.195 \times 10^6$	1,009.457	128.809	150.540	16.419
$3.190 \times 10^6$	763.951	76.152	203.191	22.161
$4.290 \times 10^6$	55.249	0.201	279.148	30.445

ducing GOR of 1.871 Mcf/STB.

TABLE 5 — PSEUDOPRESSURE,  $m(p_{ws})$ , VS SHUT-IN PRESSURE,  $p_{ws}$ 

Flow rate, $q$ , STB/D	25
Thickness, $h$ , ft	25
Producing GOR at shut-in, $R$ , Mcf/STB	1.871
Average viscosity, $\mu_o$ , cp	1.93
Average gas saturation, $\bar{S}_g$	0.12
Gas saturation at sand-face at time of shut-in, $S_g$	0.3
Average compressibility, $\bar{c}_t$ , psi <sup>-1</sup>	$4.168 \times 10^{-4}$

## EXAMPLE CALCULATION:

## 1. Permeability thickness:

$$kh = \frac{162.6 q}{m}$$

Substituting appropriate values, we obtain

TABLE 6 — SUMMARY OF BUILDUP DATA

Pressure, $p_{ws}$ (psi)	Shut-In Pseudopressure, $m(p_{ws})$ (psi/cp)	Shut-In Time, $\Delta t$ (days)	Shut-In Pressure, $p_{ws}$ (psi)	Shut-In Pseudopressure, $m(p_{ws})$ (psi/cp)
50	0.0	0	60.04	0.511
75	1.272	0.0001	93.14	2.283
100	2.664	0.0002	117.69	3.735
125	4.176	0.0003	136.18	4.943
150	7.767	0.0004	150.20	5.905
200	9.699	0.0005	170.95	7.463
225	11.686	0.001	229.13	12.023
250	13.730	0.005	355.62	23.092
275	15.835	0.01	409.87	28.558
300	18.003	0.015	440.65	31.931
325	20.237	0.02	462.28	34.432
350	22.549	0.03	493.82	38.272
375	24.965	0.05	552.53	45.847
400	27.504	0.1	609.97	53.561
425	30.174	0.15	639.49	57.639
450	32.980	0.2	659.75	60.484
500	39.039	0.25	675.24	62.680
525	42.250	0.3	687.94	64.535
550	45.512	0.5	729.40	70.773
575	48.826	0.8	769.73	77.161
600	52.195	1	783.17	79.367
625	55.620	2	824.49	86.342
650	59.102	3	848.57	90.580
675	62.644	5	878.18	95.963
700	66.296	7	897.05	99.493
725	70.085	8	911.97	102.335
750	73.989	9	917.83	103.457
775	78.012	10.6	929.99	105.803
800	82.157	21	954.45	110.579
825	86.429	30.6	970.10	113.680
850	90.831	50.6	985.85	116.837
875	95.368	70	990.08	117.689
900	100.043	80	992.63	118.203
925	104.830	90	994.31	118.543
950	109.698	100	995.44	118.771
975	114.650	140	997.27	119.138
1,000	119.688			

$$kb = \frac{162.6 (25 \text{ STB/D})}{25.2 (\text{psi/cp/log}^*)}$$

That is,

$$kb = 161.3 \text{ md-ft.}$$

2. Skin factor:

$$s = 1.151 \left[ \frac{m(p_{ws} = 1 \text{ hr}) - m(p_{wf})}{m} - \log \frac{k}{\phi \bar{c}_t \bar{\mu} r_w^2} + 3.23 \right].$$

Substituting appropriate values, we have

$$s = 1.151 \left[ \frac{41.8 \text{ psi/cp} - 0.51 \text{ psi/cp}}{25.2 \text{ psi/cp/log}^*} - \log \frac{6.45}{0.119 (1.93 \text{ cp}) (4.168 \times 10^{-4} \text{ psi}^{-1}) (0.25 \text{ ft}^2)} + 3.23 \right].$$

That is,

$$s \approx -0.64.$$

We have not taken into account that gas is flowing in the skin-factor calculation. Actually, for this situation, the GOR is fairly high.

\*\*\*